Transfer and Amplification of Cyanostilbene Molecular Function to Advanced Flexible Optical Paints Through Self-Crosslinkable Side-Chain Liquid Crystal Polysiloxanes

Journal:	*Materials Horizons*
Manuscript ID	MH-COM-01-2021-000004.R1
Article Type:	Communication
Date Submitted by the Author:	02-Mar-2021
Complete List of Authors:	Koo, Jahyeon; Chonbuk National University, Polymer-Nano Science and Technology Jang, Junhwa; Jeonbuk National University College of Engineering Lim, Seok-In; Chonbuk National University College of Engineering, Polymer-Nano Science and Technology Oh, Mintaek; Jeonbuk National University College of Engineering Lee, Kyung Min; Wright-Patterson Air Force Base McConney, Michael; Wright-Patterson Air Force Base, US Air Force Research Laboratory De Sio, Luciano; Sapienza University of Rome, Department of Medico-surgical Sciences and Biotecnologies Kim, Dae-Yoon; Korea Institute of Science and Technology, Functional Composite Materials Research Center Jeong, Kwang-Un; Jeonbuk National University College of Engineering, Department of Polymer Nano-Science and Technology

SCHOLARONE™
Manuscripts

Transfer and Amplification of Cyanostilbene Molecular Function to Advanced Flexible Optical Paints Through Self-Crosslinkable Side-Chain Liquid Crystal Polysiloxanes

Jahyeon Koo,[a] Junhwa Jang,[a] Seok-In Lim,[a] Mintaek Oh,[a] Kyung Min Lee,[b] Michae E. McConney,[b] Luciano De Sio,[c] Dae-Yoon Kim,*[d] and Kwang-Un Jeong *[a]

New Concept

Stimuli-induced color and luminescence tunable organic materials have been studied much for advanced optical applications. Among them, photoisomerizable dyes are attracting big attention because of advantages such as remote switching and photopatterning. However, the photoisomerization accompanying a large volume change is occasionally suppressed in solid state or at room temperature. To improve their practicality, the applicability range of photoisomerizable dyes need to be further extended to all cases including polymer network system. This article presents a reasonable strategy through introduction of polymethylhydrosiloxane (PMHS). A newly synthesized side-chain liquid crystal polsiloxane (Si-CSM) for advanced optical paints consists of PMHS backbone and cyanostilbene side-chain. Flexibility of PMHS backbone induces liquid crystal phase over a wide temperature range, which facilitates both photoisomerization and uniaxial orientation at room temperature. In addition, PMHS can be self-crosslinked without any crosslinker in presence of small amount of Pt catalyst. Therefore, the simplification of paint composition and the robustness of Si-CSM optical paint are simultaneously achieved. The self-crosslinked Si-CSM paint shows enhanced thermal and chemical stability, and can be bent and stretched in relatively harsh conditions. As a result, polarization-dependent and photopatternable secret coatings available for flexible objects are successfully demonstrated through photoisomerization and subsequent self-crosslinking processes.

[a].Department of Polymer-Nano Science and Technology, Department of Nano Convergence Engineering, Jeonbuk National University, Jeonju 54896, Korea. E-mail: kujeong@jbnu.ac.kr
[b].US Air Force Research Laboratory, Wright-Patterson Air Force Base, Ohio 45433, USA.
[c]. Center for Biophotonics and Department of Medico-Surgical Science and Biotechnologies, Sapienza University of Rome, Latina 04100, Italy.
[d].Functional Composite Materials Research Center, Korea Institute of Science and Technology, Jeonbuk 55324, Korea. E-mail: kdaeyoon@kist.re.kr

COMMUNICATION

Transfer and Amplification of Cyanostilbene Molecular Function to Advanced Flexible Optical Paints through Self-Crosslinkable Side-Chain Liquid Crystal Polysiloxanes

Jahyeon Koo,[a] Junhwa Jang,[a] Seok-In Lim,[a] Mintaek Oh,[a] Kyung Min Lee,[b] Michael E. McConney,[b] Luciano De Sio,[c] Dae-Yoon Kim,*[d] and Kwang-Un Jeong *[a]

A self-crosslinkable side-chain liquid crystal polysiloxane containing cyanostilbene (Si-CSM) is newly synthesized for a new generation of flexible optical paints. The photoisomerization of cyanostilbene moiety at the molecular level is transferred and amplified to the phase transition of Si-CSM, resulting in the changes of macroscopic optical properties of the Si-CSM thin film. The self-crosslinking reaction between Si-H groups in the Si-CSM polymer backbone makes the self-crosslinked Si-CSM thin film very elastic and both thermally and chemically stable. Therefore, the self-crosslinked Si-CSM thin film endures stretching and bending deformations under relatively harsh conditions. In addition, uniaxially oriented and self-crosslinked Si-CSM thin film generates linearly polarized light emission. Polarization-dependent and photopatternable secret coatings are fabricated by a spontaneous self-crosslinking reaction after coating Si-CSM paints and irradiating ultraviolet (UV) light through a photomask. The newly developed flexible optical Si-CSM paint can be applied to the next generation of optical coatings.

New Concept

Stimuli-induced color and luminescence tunable organic materials have been studied much for advanced optical applications. Among them, photoisomerizable dyes are attracting big attention because of advantages such as remote switching and photopatterning. However, the photoisomerization accompanying a large volume change is occasionally suppressed in solid state or at room temperature. To improve their practicality, the applicability range of photoisomerizable dyes need to be further extended to all cases including polymer network system. This article presents a reasonable

strategy through introduction of polymethylhydrosiloxane (PMHS). A newly synthesized side-chain liquid crystal polsiloxane (Si-CSM) for advanced optical paints consists of PMHS backbone and cyanostilbene side-chain. Flexibility of PMHS backbone induces liquid crystal phase over a wide temperature range, which facilitates both photoisomerization and uniaxial orientation at room temperature. In addition, Si-CSM can be self-crosslinked without any crosslinker in presence of small amount of Pt catalyst. Therefore, the simplification of paint composition and the robustness of Si-CSM optical paint are simultaneously achieved. The self-crosslinked Si-CSM paint shows enhanced thermal and chemical stability, and can be bent and stretched in relatively harsh conditions. As a result, polarization-dependent and photopatternable secret coatings available for flexible objects are successfully demonstrated through photo-isomerization and subsequent self-crosslinking processes.

Introduction

Color and luminescence have been studied because visual elements play a critical role in delivering information and intuitive communication. Many types of materials with various colors and emission properties are more interesting research topics than ever. Inorganic pigments and organic dyes, including metal-complex hybrids, have been synthesized and modified with the introduction of various chromophores and substituents to obtain the desired high-performance color.[1-5] In particular, multicolor properties that can be adjusted in a single molecule are attracting attention as advanced optical applications. By applying external stimuli such as thermal energy, vapor, light, pressure and electric field, the energy level of molecules with multicolor properties can be dynamically controlled.[6-10] These external stimuli induce different molecular packing, chemical reaction, phase transition, or oxidation-reduction, resulting in the variation in molecular energy levels and optical properties.

Photoisomerization of organic dyes and luminogens is one of the effective and unique ways to change both color and luminescence. Light-induced conformational changes in

a. Department of Polymer-Nano Science and Technology, Department of Nano Convergence Engineering, Jeonbuk National University, Jeonju 54896, Republic of Korea. E-mail: kujeong@jbnu.ac.kr
b. US Air Force Research Laboratory, Wright-Patterson Air Force Base, Ohio 45433, USA.
c. Center for Biophotonics and Department of Medico-Surgical Science and Biotechnologies, Sapienza University of Rome, Latina 04100, Italy.
d. Functional Composite Materials Research Center, Korea Institute of Science and Technology, Jeonbuk 55324, Republic of Korea. E-mail: kdaeyoon@kist.re.kr
† Electronic Supplementary Information (ESI) available. See DOI: 10.1039/x0xx00000x
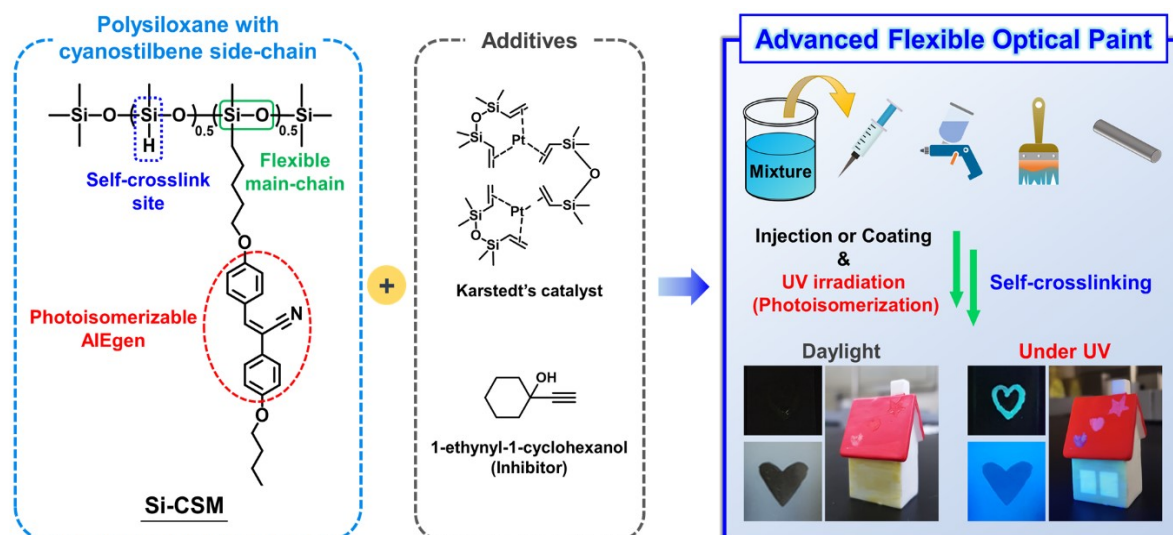
Scheme 1 Schematic illustration of the programmed Si-CSM and its application to advanced flexible optical paint.

photoisomerizable moieties can induce the dynamic changes in the molecular energy system as well as to the phase transition, which thus affects the macroscopic optical property.[11-13] Furthermore, remote-controllable patterning in specific areas can be performed by irradiating light through a photomask.[12,14,15] However, these advantages have not been exploited so far, mainly in the polymer network system. Complex molecular design and formulation is inevitable to achieve both optical changes by photoisomerization and polymer stabilization. In addition, strong molecular packing in the solid state and low molecular mobility at room temperature occasionally suppress photoisomerization.[16] Particularly, photoisomerization requiring a large volume change is more restricted in the solid state. For advanced practical applications of photoisomerizable luminogens, these limitations must be overcome.

Here, we introduce a new strategy for the development of advanced flexible optical paints (Scheme 1). The flexible optical paint is newly prepared by mixing a self-crosslinkable side-chain liquid crystal polysiloxane containing cyanostilbene (abbreviated as Si-CSM), Karstedt's catalyst, and 1-ethynyl-1-cycolhexanol (inhibitor) with an organic solvent. The newly synthesized Si-CSM consists of polymethylhydrosiloxane (PMHS) as the backbone, partially substituted cyanostilbene side chains, and residual Si-H groups in the backbone. Since the cyanostilbene moiety in the side chain is a representative aggregation-induced emission (AIE) luminogen, Si-CSM shows strong emission in the solid state. In addition, its photoisomerization of cyanostilbene moiety in the molecular level can be transferred and amplified to induce a phase transition of Si-CSM, which results in the changes of macroscopic optical properties of the Si-CSM thin film. The residual Si-H groups remaining after partial substitution of the side chains can react with each other in the presence of very small amounts of platinum catalysts, such as Karstedt's catalyst. This one-component self-crosslinking reaction significantly enhances the chemical, thermal and mechanical stability of self-crosslinked Si-CSM thin film. The flexibility of the polysiloxane

backbone not only contributes to the elastomeric mechanical properties of the self-crosslinked Si-CSM, but also allows it to have a liquid crystal (LC) phase over a wide temperature range. Additionally, the photoisomerization of Si-CSM can occur at room temperature without any trouble, and the uniaxial molecular orientation is also easily induced by mechanical shear. A small amount of inhibitor in the Si-CSM paint prevents undesirable crosslinking reactions before the coating and photopatterning process. Different solvent concentrations are used to achieve the desired viscosity for each coating process. Taken together, light-induced optical changes, and photo-patternable and polarized emissive optical coatings can be realized by a sequential process: Si-CSM paint coating - ultraviolet (UV) light irradiation through a photomask - spontaneous crosslinking by the self-crosslinking reaction.

Results and discussion

A programmed side-chain liquid crystal polysiloxane (abbreviated as Si-CSM) for advanced flexible optical paint is newly synthesized through the hydrosilylation reaction between silicon hydride group of polymethylhydrosiloxane (PMHS) and the vinyl functionalized luminogenic cyanostilbene side chain (CSM). The detailed synthetic procedures of Si-CSM and its intermediates are described in the supplementary information (Fig. S1, ESI†). The successful synthesis and purity confirmation of these compounds are conducted through proton (^{1}H), and carbon (^{13}C) NMR (Fig. S2-S5, ESI†). After the catalytic hydrosilylation reaction between PMHS and CSM, a new peak corresponding to Si-CH$_2$-C appears at 0.60 ppm, indicating that PMHS is chemically linked with CSM (Fig. S6, ESI†). On the other hand, the peak corresponding to the vinyl group of CSM disappears completely in ^{1}H-NMR spectrum.[17,18] Unreacted Si-H groups founded at 4.74 ppm are purposely left for self-crosslinking reaction and can be used to stabilize Si-CSM against external stimuli. The molar ratio of the self-crosslinking site to the photoisomerizable AIEgen is about 1:1. The

COMMUNICATION
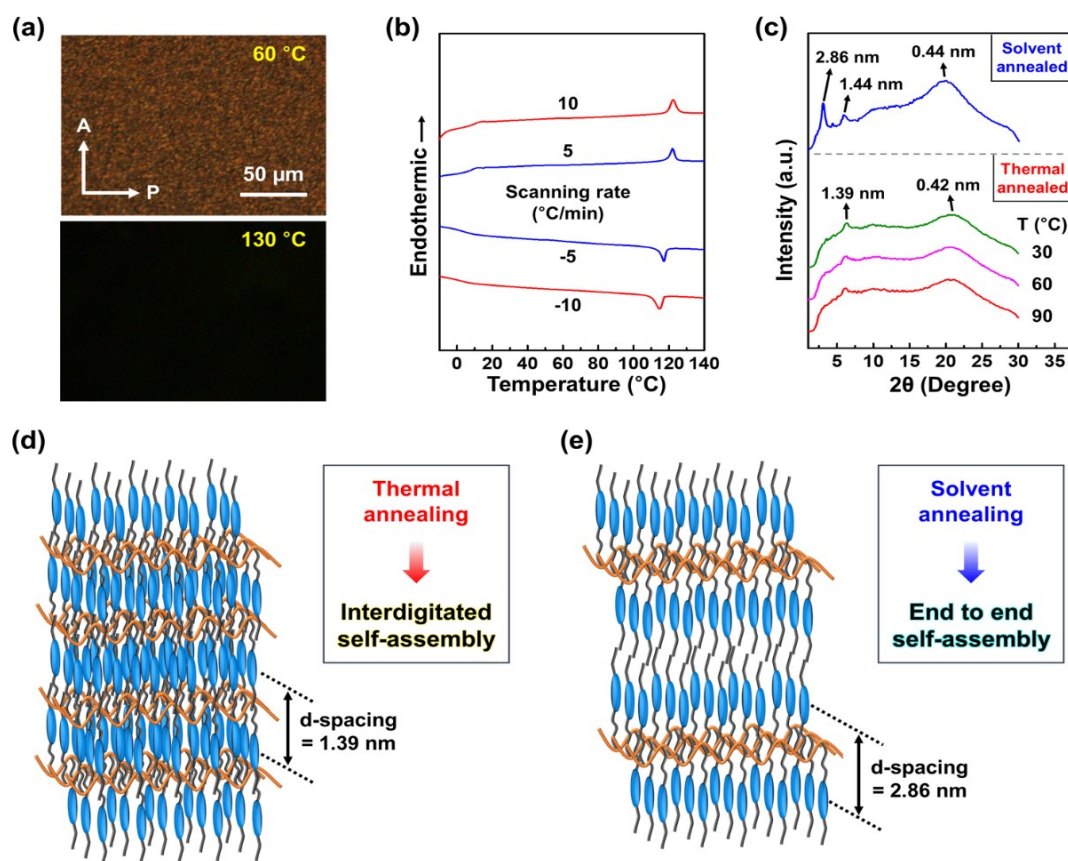
Fig. 1 Phase transition behaviors of Si-CSM: (a) POM textures at different temperatures, (b) DSC thermograms with different scanning rates, (c) 1D WAXD patterns obtained by different annealing processes, and the schematic illustrations of self-assembled structures obtained by (d) thermal and (e) solvent annealing process.

molecular weight of Si-CSM measured by gel permeation chromatography (GPC) is 10,035 g/mol (Fig. S7, ESI†), which is similar to the estimated value (9,680 g/mol) calculated from the ^{1}H-NMR spectrum of Si-CSM. In FT-IR spectrum of Si-CSM, the characteristic stretching bands of the C≡N and Si-H groups are observed at 2211 and 2165 cm^{-1}, respectively (Fig. S8, ESI†).[19,20]

The phase transition behaviors of Si-CSM are monitored by polarized optical microscopy (POM) observations at different temperatures (Fig. 1a) and differential scanning calorimetry (DSC) thermograms at different scanning rates (Fig. 1b). An endothermic peak at about 120 °C in the heating trace of DSC thermograms indicates the first order phase transition between isotropic and mesomorphic state.[21,22] A step change of heat capacity detected at around 10 °C is attributed to the glass transition temperature (T_g) of Si-CSM. The low T_g of Si-CSM is mainly due to the flexible PMHS backbone. Phase transformations can be further supported by the morphological observation on the micrometer length scale. On cooling at 5 °C/min from isotropic liquid state, the optical texture with strong birefringence is formed against the dark state, suggesting the emergence of a low-ordered liquid crystal (LC) phase. There is no noticeable change in the texture until the sample temperature is elevated above 120 °C again starting from the room temperature. The LC mesophase is maintained over a wide temperature range of 8 °C and 120 °C.[23] Additionally, the thermal degradation temperature of Si-CSM is

392 °C determined by thermogravimetric analysis (TGA) (Fig. S9, ESI†).

To investigate the self-assembly behavior of Si-CSM in detail, one dimensional (1D) wide-angle X-ray diffraction (WAXD) patterns are obtained under different annealing conditions. As can be seen in Fig. S10 (ESI†), two amorphous halos at 130 °C indicate the amorphous nature of Si-CSM. The incoherent scattering between the PMHS backbones leads to the broad halo at $2\theta = 10.60°$ (d = 0.83 nm).[24,25] The average distance of 0.44 nm ($2\theta = 20.05°$) comes from a short range positional order between cyanostilbene luminogens. When the temperature decreases from 130 °C to 110 °C, the broad scattering halo in the range $2\theta = 15° \sim 25°$ suddenly shifts to $2\theta = 21.13°$ (d = 0.42 nm), while the weak halo at $2\theta = 10.60°$ remains in the same region. A new single diffraction peak is concurrently emerged at $2\theta = 6.34°$ (d = 1.39 nm). In consideration of the first-order peak with very low intensity and no second-order peak, Si-CSM has the low-ordered smectic A (SmA) LC phase.[25,26] In addition, the calculated layer distance is much smaller than the side-chain length (l = 2.5 nm) of Si-CSM because of side-chain interdigitation.[25,26]

Since the thermal transition behaviors depending on the rate of heating and cooling process could be related with phase transformation kinetics, isothermal annealing experiments are conducted. Si-CSM in the isotropic phase is cooled to a temperature of 90, 60, or 30 °C at a rate of 5 °C/min, and then isothermally annealed at that temperature for 60 min.

However, there is no change in the 1D WAXD patterns annealed isothermally over this temperature and the above mentioned time range, as shown in Fig. 1c. This indicates that the Si-CSM shows a LC phase formed directly from the isotropic state over the wide temperature range between 8 °C and 120 °C.

Si-CSM subjected to 2 days of solvent annealing in a good solvent of chloroform exhibits multiple reflections (Fig. 1c). The peaks in a low-angle region are separated by two 2θ value, indicating lamellar structure. The primary reflection observed at $2\theta = 3.08°$ corresponds to the interlayer spacing (L) between lamellae of approximately 2.86 nm. These reflections indicate that a sublayer is only observed in the solvent annealed Si-CSM (form II, Fig. 1e), but not in the thermally annealed Si-CSM (form I, Fig. 1d). The average lateral distance of the side-chain is 0.44 nm ($2\theta = 20.03°$). The long-term solvent annealing in a good solvent can increase the chain mobility yielding improvement of recognition of nanophase separated building blocks.[27-29] Note that the phase transition between form I and II is reversible and can be repeated several cycles (Fig. S11, ESI†). The reversible change in layer spacing between 1.39 nm and 2.86 nm during the phase transition cycle by applying heat and solvent treatment are extracted by 1D WAXD. The driving force for phase transition is due to the stability difference upon thermal or solvent annealing. The form I of Si-CSM is thermodynamically stable at the temperature below isotropic state, while form II is caused by cooperative interactions with solvent. Si-CSM thus exhibits structural changes depending on the processing history. The thermally annealed Si-CSM shows smectic domains with the interdigitated molecular packing. The solvent-

annealed sample exhibits the layer structures with end-to-end self-assembly by minimized overlapping of extended butyl side chain.[29-31]

The consideration of bulk density of this LC polymer can further explain two different molecular packing modes (Fig. S12, ESI†). The density of the form I and II is measured to be 1.11 g/cm^3 and 1.08 g/cm^3, respectively. The thermally annealed Si-CSM has a slightly higher density than the solvent annealed one. The monolayer structure with the layer thickness of 1.39 nm can contain more side-chain molecules than the bilayer structure with the layer thickness of 2.86 nm under the same volume of the macroscopic pieces owing to the compact molecular packing. The proposed molecular packing models of Si-CSM obtained in different annealing processes are schematically illustrated in Figs. 1d and 1e.

The aggregation-induced emission (AIE) properties of Si-CSM are investigated by ultraviolet-visible (UV-Vis) and photo-luminescence (PL) spectrophotometers. Several Si-CSM solutions with different water fraction (f_w) of 0 to 90 are prepared, and then the absorption and PL changes are monitored (Fig. S13, ESI†). The dissolved Si-CSM in tetrahydrofuran (THF) shows the absorption band at 348 nm corresponding to the cyanostilbene moiety. By adding a large amount of water as a poor solvent, the transparent Si-CSM solution turns to cloudy due to the molecular aggregation resulting the light scattering. The absorption band is red-shifted from 348 nm to 369 nm and broaden by J-aggregation of cyanostilbene moieties in Si-CSM.[32,33] The emission band shifts gradually to longer wavelength and the intensity is increased
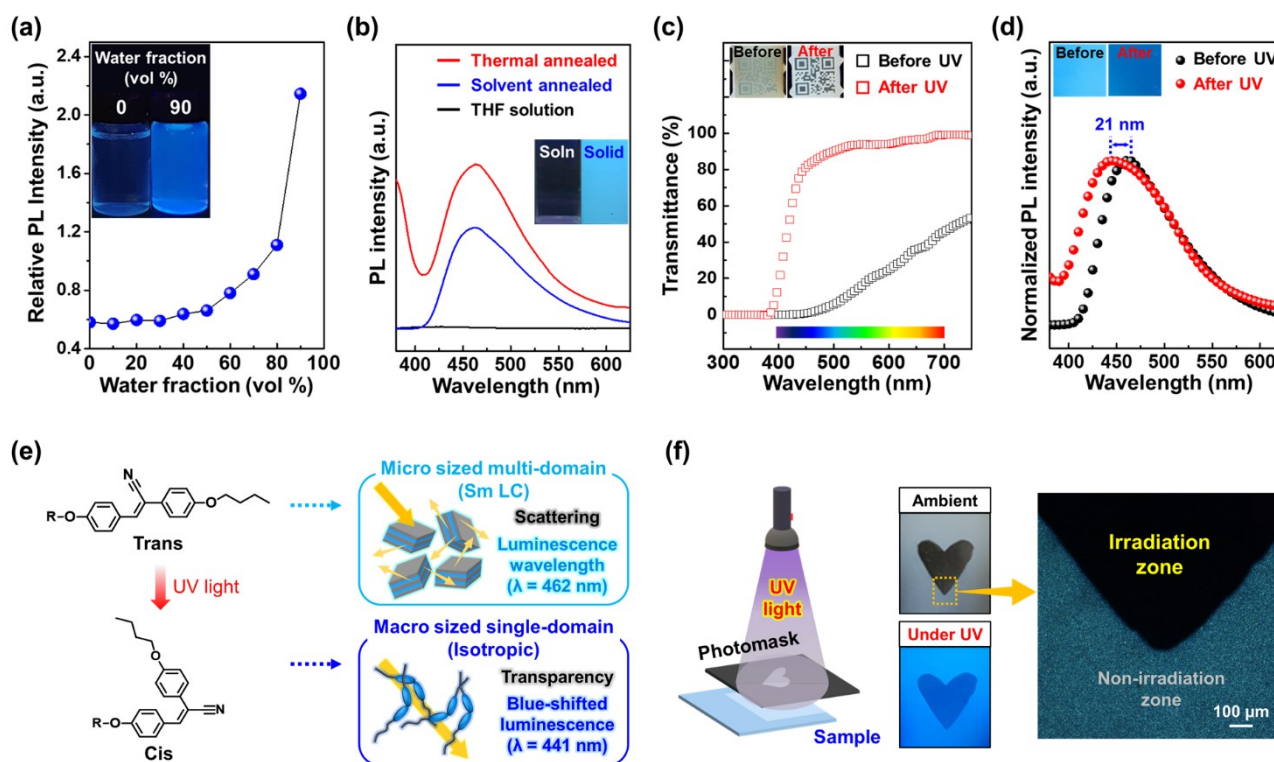

Fig. 2 Aggregation-induced emission and optical changes upon photoisomerization of Si-CSM: (a) PL intensity of Si-CSM solution (0.005 % (w/v), THF/H$_2$O) with different water fractions, (b) PL spectra of Si-CSM solution and solid films, (c) transmittance and (d) PL spectra change of Si-CSM film (thickness: 30 μm) before and after UV irradiation, (e) schematic illustration of optical changes upon photoisomerization, (f) a photopatterned heart-shaped sample and the corresponding POM texture.

upon increasing f_w (Fig. 2a and Fig. S13, ESI†). The PL intensity of Si-CSM increases slowly in aqueous mixtures when $f_w < 0.5$, while increases dramatically when $f_w > 0.5$. Obviously, the change of absorption band and greatly enhanced emission of Si-CSM by aggregation are shown. Compared to Si-CSM solution, the thin solid films also show much stronger emission at $\lambda_{max} = 462$ nm (Fig. 2b). The thin films of Si-CSM prepared by thermal or solvent annealing process have different layer-spacing in their self-assembled structures, but the emission spectra are almost identical. This indicates that the intermolecular interactions between the cyanostilbene luminogens, which mainly affect the emission properties, do not change significantly within the layer. Note that the d-spacing of cyanostilbene luminogens in the thermally annealed and solvent-annealed Si-CSM samples are 0.42 nm and 0.44 nm, respectively.

The photoisomerization of cyanostilbene group in Si-CSM is studied using ^{1}H-NMR, UV-Vis and PL measurements. After UV irradiation (365 nm wavelength, 10 mW/cm^{2}) to Si-CSM dissolved in deuterochloroform for 15 min, the two new peaks appear at 7.13 and 6.65 ppm in the ^{1}H-NMR spectrum (Fig. S14, ESI†). Two peaks (H_a', H_b') correspond to the proton of the double bond and the aromatic ring in the cis-cyanostilbene and the peak at 3.83 ppm corresponds to the proton at the H_c' position.[12,34,35] After UV irradiation under previous conditions, the absorption band of Si-CSM solution shifts to a shorter wavelength (Fig. S15a, ESI†). This blue-shift phenomenon can

be explained by the photosiomerization of the cyanostilbene group from trans to cis isomers, resulting in shorter conjugation length of luminogen.[12,34,35] As shown in Fig. S15b (ESI†), the blue-shifted emission at 390 nm is also induced. The enhanced emission efficiency is accounted for the restricted molecular rotational motion of the relatively rigid cis isomer.[36,37]

The photoisomerization behavior is also observed in Si-CSM solid films. The optical changes in the transmittance and PL spectra upon UV irradiation are represented in Fig. 2c and d. The solid film before UV irradiation shows low transmittance due to the light scattering from the micrometer sized multi-domain. Particularly low transmittance at the wavelengths below 500 nm is caused by the absorption of the self-assembled Si-CSM. After UV irradiation, the transmittance in the visible wavelength range is rapidly increased to more than 80 %. The phase transition from the smectic phase to the isotropic state is driven by photoisomerization, which results in the formation of macro-sized single domain and high transmittance of Si-CSM solid film.[13,38] As can be seen from the inset in Fig. 2c, the image of the QR code can be seen through the transparent Si-CSM film. In addition, the blue-shifted absorption of cis isomer contributes largely to the transmittance enhancement at the wavelength between 400 and 500 nm. The emission peak of the solid film shifts from 462 to 441 nm under UV irradiation, and the 21 nm blue shift of emission peak shows a change in luminescent color, as shown in the inset of Fig. 2d. The PL quantum yield of initial and photoisomerized Si-CSM is
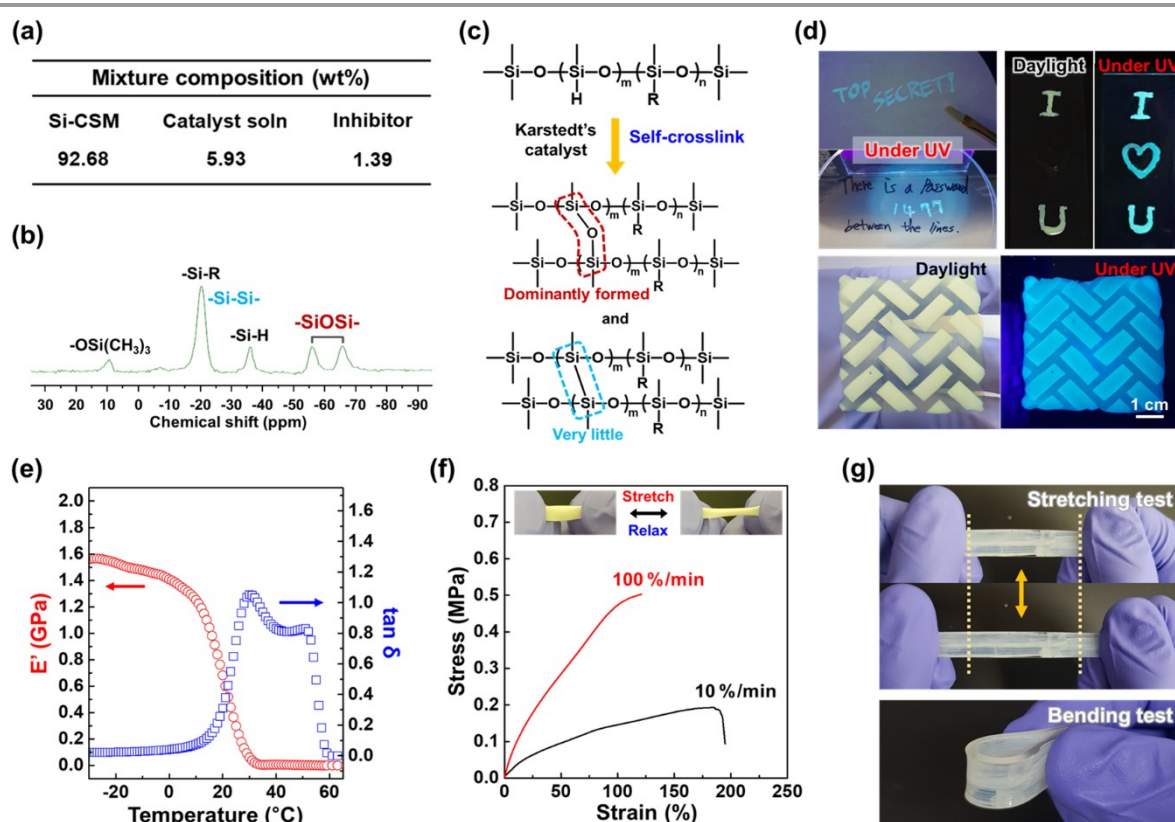
Fig. 3 Self-crosslinkable Si-CSM paint and its mechanical properties: (a) mixture composition of the well-formulated Si-CSM paint, (b) solid-state ^{29}Si-NMR spectrum of the self-crosslinked Si-CSM paint, (c) schematic diagram of self-crosslinking reaction, (d) photographs of secret and patterned coatings using Si-CSM paint, (e) DMA graph of the self-crosslinked Si-CSM film, (f) strain-stress curves of the self-crosslinked film at different strain rates, and (g) simple mechanical tests of the Si-CSM paint (thickness: 50 μm) coated on PDMS.

measured to be 1.01 % and 1.37 %, respectively (Fig. S16, ESI†). There is no significant change in quantum yield. In summary, the photoisomerization of solid state Si-CSM can be occurred easily at room temperature upon exposure to UV light and can be accompanied by optical changes in both transmittance and luminescence (Fig. 2e). Based on these characteristics, the Si-CSM films can be successfully photopatterned using a photomask. In Fig. 2f, a heart-shaped pattern shows a great contrast between the exposed and unexposed area. The exposed area is transparent and has a blue-shifted emission under UV light. The difference between exposed and unexposed area is also observed in POM images. Unlike bright textures of unexposed area, the exposed area shows no birefringence indicating the isotropic state of Si-CSM.

To prepare Si-CSM optical paint, Si-CSM is mixed with a very small amount of platinum(0)-1,3-divinyl-1,1,3,3-tetramethyl-disiloxane complex solution (Karstedt's catalyst, in xylene, Pt ~ 2 %) and 1-ethynyl-1-cyclohexanol (inhibitor). The mixture composition is shown in Fig. 3a and the detailed preparation is described in the supplementary information. The prepared Si-CSM mixture is slowly cured by self-crosslinking reaction between the Si-H groups on the polymer backbone. At room temperature, it takes several days for the paint to be fully cured. To reduce the curing time, the painted film is first cured at room temperature for 12 hours and then kept at 60 °C for 12 hours.[39,40] The crosslinking density of the film can be controlled by the amount of catalyst (Fig. S17, ESI†). There is no significant change in LC and optical properties depending on crosslinking density under the given condition (Fig. S18, ESI†). The fully cured film has a very smooth surface and shows a root mean square (RMS) roughness of 7.93 nm (Fig. S19, ESI†). With Si-CSM paint, the light-induced secret and photopatterned coatings can be easily prepared by painting, subsequent UV irradiation (transition to secret mode and photopatterning) and spontaneous curing through self-crosslinking reaction (Fig. 3d).

During the self-curing process, Si-Si and Si-O-Si crosslink bonds are created (Fig. 3c). Protons in the backbone are detached by Pt in catalyst and Si-Si bonds are formed (dehydrocoupling). Then, H and Si radicals formed by homolytical cleavage of Si-H bonds and the generated H_2 gas make Si-O-Si bond in the presence of O_2 gas (oxidation).[39,40] In ^{29}Si-NMR spectrum of Fig. 3b, Si-O-Si bonds are detected as two peaks of -56 and -66 ppm. It is difficult to find Si-Si bonds at -20 ppm because of overlap with Si atoms in Si-R bonds.[39,40] However, the presence of Si-Si bonds is confirmed in the ^{29}Si-NMR spectrum of self-crosslinked PMHS (Fig. S20, ESI†). The Si-Si bond at -20 ppm is clearly observed due to the absence of Si-R bonds in PMHS. In a return to Fig. 3b, unreacted Si-H groups after self-crosslinking are observed at -36 ppm. Considering the integration of respective peaks in the spectrum, Si-O-Si bond is dominantly formed. It may be related to self-crosslinking mechanism and reaction kinetics. The crosslinking of the self-crosslinked film is further confirmed by the enhanced thermal stability and chemical resistance. The self-crosslinked Si-CSM paint film does not flow at 180 °C, which is much higher than the melting point (120 °C) of Si-CSM (Fig. S21a and b, ESI†). The thermal degradation of the self-crosslinked film begins to occur above 363 °C, as shown in Fig. S21c (ESI†). The crosslinked Si-CSM paint starts to decompose at a temperature slightly below the degradation point of pure Si-CSM because Si-CSM paint contains a small amount of additives including catalyst and inhibitor.[41] After removing impurities with acetone, the degradation temperature of the crosslinked film increases to 379 °C. The self-crosslinked film does not dissolve after rinsing with chloroform or immersion in acetone for 30 min (Fig. S22, ESI†). Due to the self-crossliking, Si-CSM paint film can retain its shape at high temperature as well as against the chemical attacks.

The mechanical properties of the self-crosslinked Si-CSM films are examined by dynamic mechanical analysis (DMA) and tensile tests. As shown in Fig. 3e, the storage modulus in the glassy state below 0 °C is above 1.4 GPa. With increasing temperature, the modulus decreases to tens of MPa above 10 °C, the T_g of the film. At around 55 °C, the further decrease in storage modulus occurs due to the phase transition from smectic to nematic LC phase.[42,43] Accordingly, the loss tangent (tan δ) exhibits two peaks at 29 °C and 53 °C. These results are in good agreement with DSC and 1D WAXD data of the crosslinked film (Fig. S23, ESI†). In addition, the nematic to isotropic phase transition (T_{NI}) of the film occurs at 113 °C.

As shown in Fig. 3f, the self-crosslinked Si-CSM film shows that reversible stretching and relaxation behavior is possible within about 100 % strain due to the partially crosslinked and flexible polysiloxane backbone. Under different strain rates of 10 %/min and 100 %/min at 25 °C, the film breaks at 184 % and 121 % strain, and its tensile strength is 0.19 MPa and 0.50 MPa.
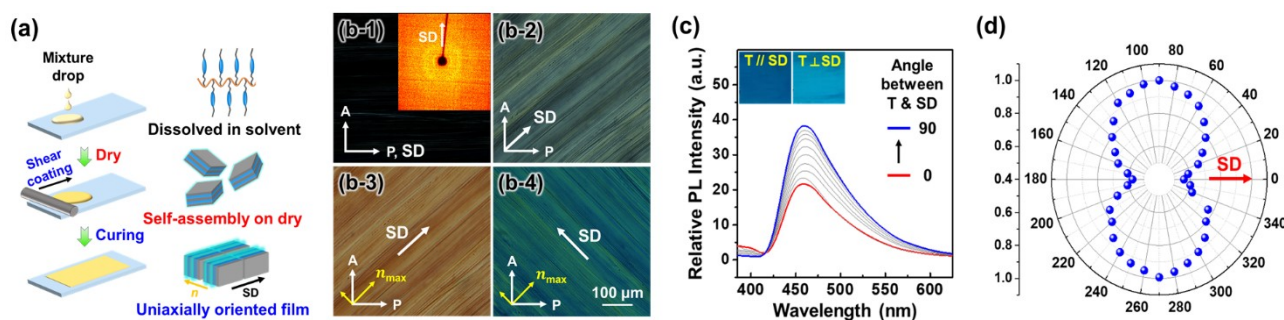

Fig. 4 The shear-induced uniaxially oriented Si-CSM coatings: (a) schematic illustrations of shear-induced orientation, (b) POM observations with a retardation plate (inset figure is a 2D WAXD pattern of the oriented film), (c) polarized PL spectra, and (d) PL intensity as a function of the angle between shear direction (SD) and transmittance (T) axis of a polarizer.

The mechanical and fracture properties of most polymers depend on the applied strain rate due to their viscoelasticity.[44] Based on its mechanical properties, Si-CSM paint can be coated and applied to flexible objects. As shown in Fig. 3g, Si-CSM paint coated on PDMS film shows stable stretching and bending behavior. It is not broken during several bending and stretching tests. Furthermore, the undesirable changes in the emission color of the crosslinked Si-CSM during stretching and relaxing are not detected although it has been reported that some AIE luminogen-based polymers have mechanochromic property (Fig. S24a, ESI†).[45,46] The emission spectra of the stretched and relaxed Si-CSM film exhibit almost the same PL spectra. As shown in Fig. S24b and c (ESI†), any distinct structural changes and orientation of the self-assembled structures are not observed from the POM and WAXD results. Therefore, the emission properties of the self-crosslinked Si-CSM paint are well-maintained under mechanical loads, a positive phenomenon in terms of general painting applications.

Applying shear force to the drop-casted and dried Si-CSM paints yields uniaxially oriented thin films, which is caused by the high molecular mobility of Si-CSM at room temperature (Fig. 4a). The oriented and subsequently cured film with a thickness of 20 µm is used for this study. As shown in Fig. 4b, the sheared sample shows birefringence as a function of the angle between shear direction (SD) and polarizer axis. Dark and maximum bright images are observed when the SD and polarizer axis are 0° and 45°, indicating that the self-assembled structure formed upon drying is uniaxially oriented by the shear force.[47] The 2D WAXD image in Fig. 4b-1 also supports the uniaxially oriented and self-assembled structure of the sheared Si-CSM paint. Since Si-CSM is annealed by the solvent through the solution casting and drying process, first and second order diffractions are observed at the equator, indicating that the layer normal is perpendicular to the SD.[48,49] The molecular arrangement is further identified by POM observations with a 530 nm retardation plate (Fig. 4b-3 and -4). When the SD and the slow axis of the retardation plate are parallel, a yellowish POM image is observed due to the retardation subtraction.[47] When the SD and the slow axis are perpendicular, a blueish POM image is appeared by addition effect. It is concluded that the long axis of cyanostilbene is perpendicular to the SD and layer.

Before measuring the linearly polarized emission property, the polarized absorption of the uniaxially oriented Si-CSM film is confirmed (Fig. S25, ESI†). The maximum absorption occurs in the perpendicular condition between the SD and transmittance axis (T) of a polarizer. On the other hand, the minimum absorption spectrum is represented when the SD and T are parallel. Likewise, the PL spectra of the uniaxially oriented Si-CSM film show the polarized emission behaviors (Fig. 4c and d). The PL intensity gradually increases as the angle between the SD and T increases from parallel (0°) to perpendicular (90°). The obvious contrast between maximum and minimum intensity is shown in the inset of Fig. 4c. The calculated polarization ratio of $P = I_{\parallel}/I_{\perp}$ is 1.79 and the order parameter of $S = (I_{\parallel} - I_{\perp})/(I_{\parallel} + 2I_{\perp})$ is 0.21, where $I_{\parallel}$ and $I_{\perp}$ are the maximum PL intensities in parallel and perpendicular conditions between SD and T.[41] The somewhat low P and S values may be originated from some defects in the shear-coated Si-CSM paint and the attenuated orientational order caused by self-crosslinking reaction.[50,51] Note that the measured polarization ratio (P) of the shear coated film before self-crosslinking reaction is 2.10 (Fig. S26, ESI†). However, the sufficiently different PL intensity according to the angle between SD and T can make different optical signals in polarized paint applications.

Utilizing light-induced optical change behavior, flexible mechanical properties, shear-induced orientation of Si-CSM paint, a variety of advanced flexible optical coatings are demonstrated. After painting and photopatterning in certain areas, the UV exposed areas are invisible under ambient light and show a different luminescence color under UV light as
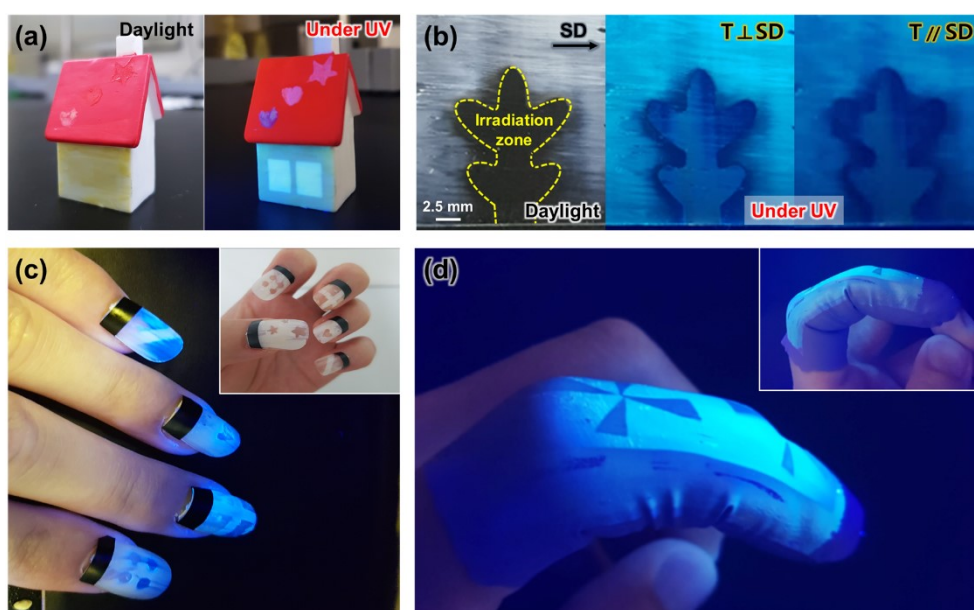

Fig. 5 Demonstration of the advanced flexible optical coatings using Si-CSM paints: (a) the decorated miniature house, (b) the photopatterned and polarized emissive coating, the patterned (c) artificial nails and (d) rubber glove.

shown in Fig. 5a. In Fig. 5c, the programmed artificial nails fabricated with Si-CSM paint are introduced. The polarized light emissive coatings are also obtained by applying shear force to the drop casted and dried paint (Fig. 5b). Subsequent UV irradiation through a photomask also leads to the optical changes in certain areas and the UV exposed areas do not exhibit polarized emission properties due to the loss of molecular orientational order through photoisomerization. By combining shear-induced polarized emission and photo-patterning of transmittance and luminescence, dual-mode optical patterns can be easily realized with a polarizer. Furthermore, Si-CSM paint can be applied to flexible objects because of its elastomeric properties. As shown in Fig. 5d, the painted and subsequently photopatterned nitrile glove displays the programmed optical patterns. The paint on the glove is robust in both mechanical and optical properties during repetitive flexion and extension of a finger.

Conclusions

The programmed Si-CSM was newly synthesized for the developement of advanced flexible optical paints. The Si-CSM film showed strong emission at 462 nm because of the AIE property of the cyanostilbene side chain. Because the flexible backbone of Si-CSM allowed the formation of low-ordered smectic A (SmA) LC phase over a wide temperature range between 8 °C and 120 °C, Si-CSM can be easily photoisomerized and oriented even at room temperature. The UV-irradiated Si-CSM film exhibited a highly enhanced transmittance and blue-shifted emission at 441 nm due to the photoisomerization of the cyanostilbene moiety. The uniaxially oriented and self-crosslinked Si-CSM thin film emitted linearly polarized light. Also, the self-crosslinked Si-CSM thin film can be bent and stretched because of its high elasticity and strong mechanical stability, which are resulted from the self-crosslinking reaction between Si-H groups in the Si-CSM backbone. By combining the light-induced optical change behavior and shear-induced polarized emission property of the Si-CSM paint, photopatternable and polarized light emissive coatings were achieved. The proposed Si-CSM paint can be applied in security and advanced optical coatings for flexible objects and soft actuators.

Conflicts of interest

There are no conflicts to declare.

Acknowledgements

Notes and references

1   S. Jin, G. Cheng, G. Z. Chen, Z. Ji, *J. Porphyrins Phthalocyanines*, 2005, **9**, 32.
2   S. Redon, G. Eucat, M. Ipuy, E. Jeanneau, I. Gautier-Luneau, A. Ibanez, C. Andraud, Y. Bretonniere, *Dyes and Pigments*, 2018, **156**, 116.
3   B. K. Bera, C. Chakraborty, S. Malik, *J. Mater. Chem. C*, 2017, **5**, 6872.
4   A. Maron, A. Szlapa, T. Klemens, S. Kula, B. Machura, S. Krompiec, J. G. Matecki, A. Switlicka-Olszewska, K. Erfurt, A. Chrobok, *Org. Biomol. Chem.*, 2016, **14**, 3793.
5   B. Bonillo, R. S. Sprick, A. I. Cooper, *Chem. Mater.*, 2016, **28**, 3469.
6   X. Zhang, Z. Chi, Y. Zhang, S. Liu, J. Xu. *J. Mater. Chem. C*, 2013, **1**, 3376.
7   J. P. Lee, H. Hwang, S. Chae, J.-M. Kim, *Chem. Commun.*, 2019, **55**, 9395.
8   N. Sun, K. Su, Z. Zhou, X. Tian, Z. Jianhua, D. Chao, D. Wang, F. Lissel, X. Zhao, C. Chen, *Macromolecules*, 2019, **52**, 5131.
9   Z. Li, Y. Xie, M. Zhu, Y. Song, M. Qin, X. Hu, *Optical Materials*, 2019, **94**, 257.
10 D.-Y. Kim, J. Koo, S.-I. Lim, K.-U. Jeong, *Adv. Funct. Mater.*, 2018, **28**, 1707075.
11 M. Shi, J. Mack, L. Yin, X. Wang, Z. Shen, *J. Mater. Chem. C*, 2016, **4**, 7783.
12 J. Seo, J. W. Chung, J. E. Kwon, S. Y. Park, *Chem. Sci.*, 2014, **5**, 4845.
13 D.-Y. Kim, S.-A. Lee, H. Kim, S. M. Kim, N. Kim, K.-U. Jeong, *Chem. Commun.*, 2015, **51**, 11080.
14 A. Abdollahi, H. Alidaei-Sharif, H. Roghani-Mamaqani, A. Herizchi, *J. Mater. Chem. C*, 2020, **8**, 5476.
15 J. R. Talukder, H.-Y. Lin, S.-T. Wu, *Optics Express*, 2019, **27**, 18169.
16 A. Gonzalez, E.S. Kengmana, M.V. Fonseca, G.G.D. Han, *Materials Today Advances*, 2020, **6**, 100058.
17 N. A. A. Rossi, E. J. Duplock, J. Meegan, D. R. T. Roberts, J. J. Murphy, M. Patel, S. J. Holder, *J. Mater. Chem.*, 2009, **19**, 7674.
18 F.-B. Meng, Y. Cui, H.-B. Chen, B.-Y. Zhang, C. Jia, *Polymer*, 2009, **50**, 1187.
19 Y. Zhang, C. Liang, H. Shang, Y. Ma, S. Jiang, *J. Mater. Chem. C*, 2013, **1**, 4472.
20 H.W. Bai, G. Wen, X.X. Huang, Z.X. Han, B. Zhong, Z.X. Hu, X.D. Zhang, *J. Eur. Ceram. Soc.*, 2011, **31**, 931.
21 D.-G. Kang, H. Ko, J. Koo, S.-I. Lim, J. S. Kim, Y.-T. Yu, C.-R. Lee, N. Kim, K.-U. Jeong, *ACS Appl. Mater. Interfaces*, 2018, **10**, 35557.
22 D.-Y. Kim, S.-A. Lee, Y.-J. Choi, S.-H. Hwang, S.-W. Kuo, C. Nah, M.-H. Lee, K.-U. Jeong, *Chem. Eur. J.*, 2014, **20**, 5689.
23 L. Zhang, W. Yao, Y. Gao, C. Zhang, H. Yang, *Polymers*, 2018, **10**, 794.
24 D.-Y. Kim, M. Park, S.-A. Lee, S. Kim, C.-H. Hsu, N. Kim, S.-W. Kuo, T.-H. Yoon, K.-U. Jeong, *Soft Matter*, 2015, **11**, 58.
25 A. Sarkar, M. Mehra, D. Dasgupta, L. Negi, A. Saxena, *Macromolecules*, 2018, **51**, 9354.
26 W. Yao, Y. Gao, W. Yuan, B. He, H. Yu, L. Zhang, Z. Shen, W. He, Z. Yang, H. Yang, D. Yang, *J. Mater. Chem. C*, 2016, **4**, 1425.
27 H. Iino, J.-I. Hanna, *Polymer Journal*, 2017, **49**, 23.
28 D.-Y. Kim, D.-G. Kang, S. Shin, T.-L. Choi, K.-U. Jeong, *Polym. Chem.*, 2016, **7**, 5304.
29 Y. Wang, H. Cui, M. Zhu, F. Qiu, J. Peng, Z. Lin, *Macromolecules*, 2017, **50**, 9674.

30 K. Ebata, Y. Hashimoto, S. Yamamoto, M. Mitsuishi, S. Nagano, J. Matsui, *Macromolecules*, 2019, **52**, 9773.

31 S. Liang, Y. Xu, C. Li, J. Li, D. Wang, W. Li, *Polym. Chem.*, 2019, **10**, 4584.

32 Y. Yuan, J. Li, L. He, Y. Liu, H. Zhang, *J. Mater. Chem. C*, 2018, **6**, 7119.

33 Y. Ma, M. Cametti, Z. Dzolic, S. Jiang, *J. Mater. Chem. C*, 2016, **4**, 10786.

34 M. Martinez-Abadia, S. Varghese, R. Gimenez, M. B. Ros, *J. Mater, Chem, C*, 2016, **4**, 2886.

35 Z. Ding, Y. Ma, H. Shang, H. Zhang, S. Jiang, *Chem. Eur. J.*, 2019, **25**, 315.

36 L. Zhu, C. Y. Ang, X. Li, K. T. Nguyen, S. Y. Tan, H. Agren, Y. Zhao, *Adv. Mater.*, 2012, **24**, 4020.

37 Y. Zhu, M. Zheng, Y. Tu, X.-F. Chen, *Macromolecules*, 2018, **51**, 3487.

38 S.-W, Oh, S.-H. Kim, T.-H. Yoon, *J. Mater. Chem. C*, 2018, **6**, 6520.

39 K. V. Deriabin, E. K. Lobanovskaia, A. S. Novikov, R. M. Islamova, *Org. Biomol. Chem.*, 2019, **17**, 5545.

40 K. V. Deriabin, E. K. Lobanovskaia, S. O. Kirichenko, M. N. Barshutina, P. E. Musienko, R. M. Islamova, *Appl Organometal Chem.*, 2020, **34**, e5300.

41 J. Koo, S.-I. Lim, S. H. Lee, J. S. Kim, Y.-T. Yu, C.-R. Lee, D.-Y. Kim, K.-U. Jeong, *Macromolecules*, 2019, **52**, 1739.

42 Z. Wen, M. K. McBride, X. Zhang, X. Han, A. M. Martinez, R. Shao, C. Zhu, R. Visvanathan, N. A. Clark, Y. Wang, K. Yang, C. N. Bowman, *Macromolecules*, 2018, **51**, 5812.

43 M. O. Saed, R. H. Volpe, N. A. Traugutt, R. Visvanathan, N. A. Clark, C. M. Yakacki, *Soft Matter*, 2017, **13**, 7537.

44 H. Wang, W. Deng, H. Wu, A. Pi, J. Li, F. Huang, *Defence Technology*, 2019, **15**, 875.

45 T. Han, L. Liu, D. Wang, J. Yang, B. Z. Tang, *Macromol. Rapid. Commun.*, 2020, 2000311.

46 A. Pucci, *Sensors*, 2019, **19**, 4969.

47 P. Im, D.-G. Kang, D.-Y. Kim, Y.-J. Choi, W.-J. Yoon, M.-H. Lee, I.-H. Lee, C.-R. Lee, K.-U. Jeong, *ACS Appl. Mater. Interfaces*, 2016, **8**, 762.

48 D. Shi, W.-Y. Chang, X.-K. Ren, S. Yang, E.-Q. *Chen, Polym. Chem.*, 2020, **11**, 4749.

49 J. Geng, X. Zhao, E. Zhou, G. Li, J. W. Y. Lam, B. Z. Tang, *Polymer*, 2003, **44**, 8095.

50 R. He, E. Oh, Y. Ye, P. Wen, K.-U. Jeong, S. H. Lee, X.-D. Li, M.-H. Lee, *Polymer*, 2019, **176**, 51.

51 V. K. Baliyan, V. Kumar, J. Kim, S.-W, Kang, *Opt. Mater. Express*, 2016, **6**, 2956.